Spectroscopic Studies of Stellacyanin, Plastocyanin, and Azurin. Electronic Structure of the Blue Copper Sites

Edward I. Solomon,*[1a] Jeffrey W. Hare, David M. Dooley, John H. Dawson, Philip J. Stephens,[1b] and Harry B. Gray*

Contribution No. 5992 from the Arthur Amos Noyes Laboratory of Chemical Physics, California Institute of Technology, Pasadena, California 91125. *Received March 19, 1979*

Abstract: Low-temperature absorption and room temperature circular dichroism and magnetic circular dichroism spectral studies of the blue copper proteins *Rhus vernicifera* stellacyanin, bean plastocyanin, and *Pseudomonas aeruginosa* azurin have been made. Low-energy bands attributable to d–d transitions in a flattened tetrahedral (D_{2d}) copper(II) center are observed in the near-infrared CD spectra at 5000, 9150, and 11 200 cm^{-1} in plastocyanin, 5250, 8100, and 10 500 cm^{-1} in stellacyanin, and 5800 and 10 200 cm^{-1} in azurin. Bands in the near-infrared MCD spectra are at 10 600, 8800, and 10 500 cm^{-1} in plastocyanin, stellacyanin, and azurin, respectively. The low energies of these bands rule out tetragonal six- or five-coordinate as well as square-planar four-coordinate structures, and trigonal four or five coordination is inconsistent with the blue copper EPR parameters. The band positions accord well with ligand field calculations based on a tetrahedral structure that is distorted approximately 6° toward a square plane ($^2B_2$ ($d_{x^2-y^2}$) ground state), the predicted transitions being $^2B_2 \rightarrow {}^2E$, $^2B_2 \rightarrow {}^2B_1$, and $^2B_2 \rightarrow {}^2A_1$, in order of increasing energy. EPR parameters for the three blue proteins calculated using this ligand field model are in reasonable agreement with the observed values. Ligand field stabilization energy contributions to the reduction potentials have been calculated; azurin, plastocyanin, and stellacyanin are destabilized by 250, 345, and 340 mV, respectively, relative to the aquo Cu(II) ion. Based on a comparison of absorption and CD intensities, the characteristic bands at about 13 000, 16 000, and 22 000 cm^{-1} in the blue proteins are assigned to the ligand to metal charge transfer transitions $\pi S(Cys) \rightarrow d_{x^2-y^2}$, $\sigma S(Cys) \rightarrow d_{x^2-y^2}$, and $\pi N(His) \rightarrow d_{x^2-y^2}$, respectively, in a flattened tetrahedral Cu(II) unit.

The once puzzling physical properties of blue copper proteins[2] are beginning to be understood. Evidence that progress has been made comes from recent absorption, circular dichroism (CD), and magnetic circular dichroism (MCD) spectroscopic experiments on *Rhus vernicifera* stellacyanin,[3] *Pseudomonas aeruginosa* azurin,[3] bean plastocyanin,[3] tree and fungal laccase,[4] and ceruloplasmin,[5] as in these cases the results have been interpreted successfully in terms of the electronic energy levels derived for a tetragonally (D_{2d}) distorted tetrahedral blue copper site.[3] These and other[6-8] spectroscopic studies have suggested the probable ligand composition of such a distorted tetrahedral site. In the specific case of poplar plastocyanin, an X-ray crystal structure analysis (2.7-Å resolution) has established[9] that its blue copper is bound to two nitrogen and two sulfur donors in a distorted tetrahedral geometry. The copper ion is coordinated by a cysteine thiolate, a methionine thioether group, and two histidine imidazole nitrogens. A 3-Å resolution electron density map also has been determined for *P. aeruginosa* azurin.[10] Although phasing was difficult and the resulting map noisy, the copper ion could be located and the probable ligands identified via use of the amino acid sequence. Once again, the ligating amino acids are cysteine, two histidines, and a methionine, and the copper-site geometry appears to be close to tetrahedral. Recent X-ray absorption spectroscopic measurements have shown[11] that the Cu–S(thiolate) bond distance is relatively short (2.10 ± 0.02 Å), which is consistent with a near-tetrahedral geometry. Thus all the evidence now available suggests that the structures of the blue copper sites in plastocyanin and azurin are remarkably similar; however, at least one ligand at the copper center in stellacyanin must be different, as this protein does not contain methionine.[12]

We have now completed a comprehensive spectroscopic investigation of stellacyanin, bean plastocyanin, and *P. aeruginosa* azurin. The measurements that have been made include variable temperature visible and near-infrared absorption and room temperature near-infrared and visible CD and MCD spectra for the three proteins. An analysis of site symmetry effects on Cu(II) EPR parameters has also been performed. We report in this paper a detailed formulation of the ground-state electronic structures as well as complete d–d and charge transfer transition assignments for the blue copper sites in stellacyanin, plastocyanin, and azurin.

Experimental Section

French bean (*Phaseolus vulgaris*) plastocyanin,[13] *Pseudomonas aeruginosa* azurin,[14] and *Rhus vernicifera* stellacyanin[15] were purified by standard methods. Protein concentrations were determined from absorption spectral measurements in the 600-nm region.[2,8d] Near-infrared absorption spectra were obtained on protein films to minimize interference by water absorption and permit a wide variation of temperature. The protein solutions were first dialyzed against deionized, distilled water and then concentrated from roughly 10 to 0.5 mL by membrane ultrafiltration (Amicon). The sample was then further concentrated by placing a drop of protein solution on a Plexiglas disk in a metal desiccator over Drierite. After 3 or 4 drops had been successively concentrated (10 to 15 for the thick films), the film was prepared by transferring the disk to a desiccator containing a saturated potassium acetate solution. This controlled humidity allowed the film to form slowly, thereby preventing most of the cracking caused by rapid removal of excess water. The drying process was halted by transfer to a desiccator charged with a saturated sodium hydrogen phosphate solution. The humidity of this desiccator allowed slow dissolution of the sample. Films that had been overdried were redissolved by placing them in the sodium phosphate humidifier. Whereas stellacyanin and azurin appeared unaffected by complete drying and redissolving, plastocyanin never completely redissolved. The undissolved plastocyanin was white, indicating partial denaturation upon complete removal of water. The plastocyanin samples used in the present study, therefore, were never allowed to dry past the elastic film form.

A lightly greased silicone gasket was placed on the plastic disk and a second disk placed over the gasket to prevent further drying upon evacuation in a cryocooler unit. The sample was masked with aluminum foil to prevent light leakage and to improve thermal contact with the cold station. The sample was then slowly cooled to minimum temperature. If cracks developed, the unit was warmed to near room temperature, slices of black masking tape were applied to cover large cracks, and the unit was then recooled. Plexiglas ($\frac{1}{2}$ in. diameter by $\frac{1}{32}$ in. thick) was chosen over quartz despite poorer optical quality (weak vibrational overtones at 1250 nm and longer wavelengths) because the thermal contraction more closely matched that of the protein film.

The near-infrared CD and MCD spectra were run in D_2O or deuterated phosphate buffer in order to extend the spectral range to 2000

0002-7863/80/1502-0168$01.00/0 © 1980 American Chemical Society

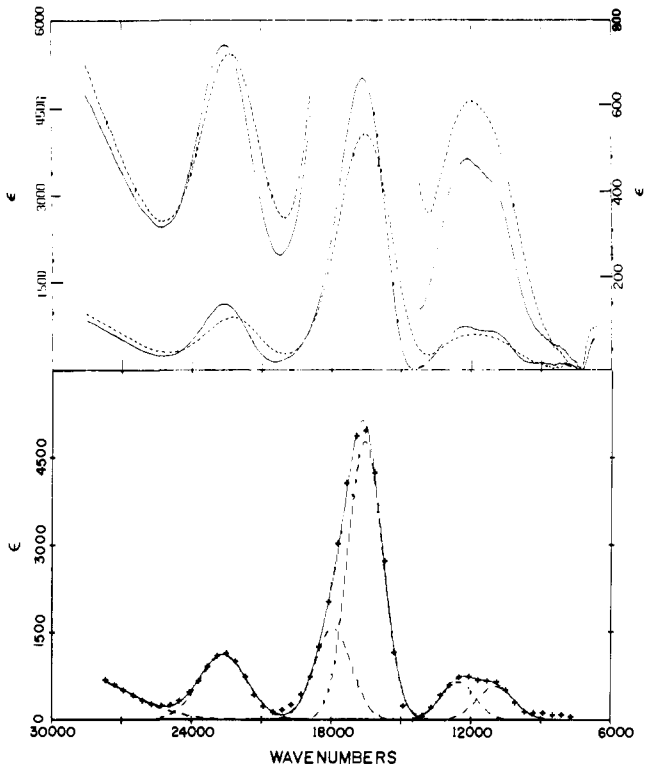

Figure 1. Top frame: the near-infrared and visible absorption spectra of stellacyanin films at 270 (- - - -) and 35 K (—); lower curves, left-hand scale; upper curves (thick film), right-hand scale. Bottom frame: Gaussian resolution of the 35 K near-infrared and visible absorption spectrum of a stellacyanin film; the symbols (+) represent the experimental absorption spectrum.

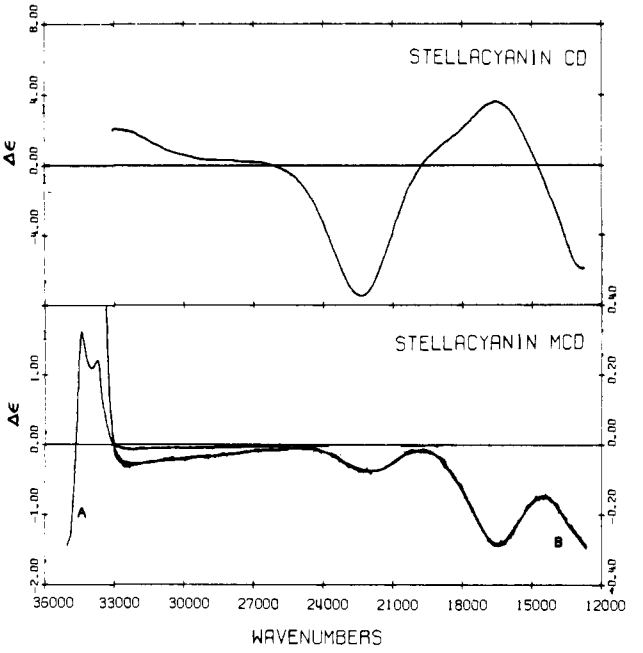

Figure 2. Top frame: the visible CD spectrum of 0.206 mM stellacyanin in pD 6 deuterated phosphate buffer at 290 K. Bottom frame: the visible MCD spectrum of 0.206 mM stellacyanin in pD 6 deuterated phosphate buffer at 290 K; curve A, left-hand scale; curve B, right-hand scale.

nm. Although the infrared overtones of water do not give rise to a measurable CD or MCD spectrum, they decrease instrumental sensitivity. Equilibration of azurin and plastocyanin samples with D_2O was carried out by concentrating the protein solutions in an Amicon ultrafiltration cell (UM-2 membrane) and then adding approximately a tenfold excess of D_2O and repeating the procedure four to five times before concentrating the solution to its final value. Stellacyanin was equilibrated with deuterated 0.5 M phosphate buffer by twice evaporating a solution to a film and then equilibrating with D_2O overnight; a film was then prepared a third time and dissolved in a minimum volume of buffer. Sample concentrations were 1.06, 3.54, and 3.56 mM for stellacyanin, plastocyanin, and azurin, respectively. Solutions for the visible CD and MCD spectra were prepared by diluting the solutions prepared for near-infrared studies with deuterated phosphate buffer of D_2O until absorbance less than 1.0 was recorded for the 600-nm band. The final concentrations were 0.206, 0.210, and 0.197 mM for stellacyanin, azurin, and plastocyanin, respectively.

The absorption spectra were obtained on a Cary 17I spectrometer. The spectra were run at constant slit widths of 0.8 mm for $\lambda < 750$ nm and 0.4 mm for $\lambda > 750$ nm. Wavelength variations in lamp output, monochromator transmission, and detector response, which are normally compensated by the slit feedback mechanism, were corrected by a feedback system on the source voltage supply that was installed by Dr. G. R. Rossman. Higher resolution measurements (0.1-mm slit width in the near-infrared) revealed no fine structure at low temperatures. The samples were cooled by a Cryogenics Technology, Inc., Model 20 cryocooler equipped with quartz windows and a temperature controller that allowed adjustment of the temperature to ±1 K over most of the range used.

The visible CD and MCD spectra were recorded on a Cary 61 spectropolarimeter. The near-infrared CD and MCD spectra were recorded on an instrument built at the University of Southern California and described elsewhere.[16] A field of 40 kG was supplied by a Varian superconducting electromagnet. Instrument base lines were determined using deuterated phosphate buffer or D_2O as a blank.

Spectra are reported in terms of molar extinction coefficient ϵ (absorption) or differential molar extinction coefficient $\Delta\epsilon$ (CD and MCD). In the case of MCD, $\Delta\epsilon$ is normalized to a field of +10 kG.

Results

The 270 K absorption spectrum of a stellacyanin film from 28 000 to 7000 cm^{-1} is consistent with solution data reported by Peisach et al.[17] A new band at approximately 8800 cm^{-1} is partially resolved when a thick film is cooled to 35 K (Figure 1). Gaussian-resolved bands from the 35 K spectrum of stellacyanin are also shown in Figure 1. The position, intensity (ϵ), half-width at half-maximum (hwhm), and oscillator strength (f) of each of the resolved Gaussian peaks as a function of temperature are given in Table I.

Our visible CD curve for stellacyanin (Figure 2) accords well with the spectrum reported by Falk and Reinhammar.[18] The MCD curve (Figure 2), which has not been reported previously, shows bands at 16 500 and 22 000 cm^{-1}. The intense bands beginning at 33 000 cm^{-1} are probably attributable to tryptophan residues, by analogy to the interpretation of the MCD curves of azurin in this energy region.[19] The near-infrared CD spectrum of stellacyanin is shown in Figure 3. Bands are observed at 10 500, 8100, and in the region of 5000 cm^{-1}. The whole of the latter band cannot be observed because of D_2O vibrational absorption. The MCD curve (Figure 3) in the near-infrared shows positive and negative features at ~10 800 and 8800 cm^{-1}, respectively. Correlation of the near-infrared (Figure 3) and visible (Figure 2) MCD spectra reveals an additional negative feature in the 13 000-cm^{-1} region.

Electronic absorption spectra of French bean plastocyanin films are presented in Figure 4. The 270 K spectrum is similar to that reported for *Chenopodium album* plastocyanin.[20] The major absorption band has a maximum at 16 700 cm^{-1} and is assigned the solution ϵ of 4500.[21] Peaks are also observed at 12 900 and 21 800 cm^{-1}. The weak, high-energy band shows considerable asymmetry in the thick film spectrum (B), and a shoulder is resolved (~24 000 cm^{-1}) at 35 K. As the film is cooled, all the bands narrow and increase in intensity. The decreasing breadth of the 12 900-cm^{-1} peak reveals residual intensity at roughly 10 000 cm^{-1}. A band at this low energy has not previously been observed. Figure 4 also shows the

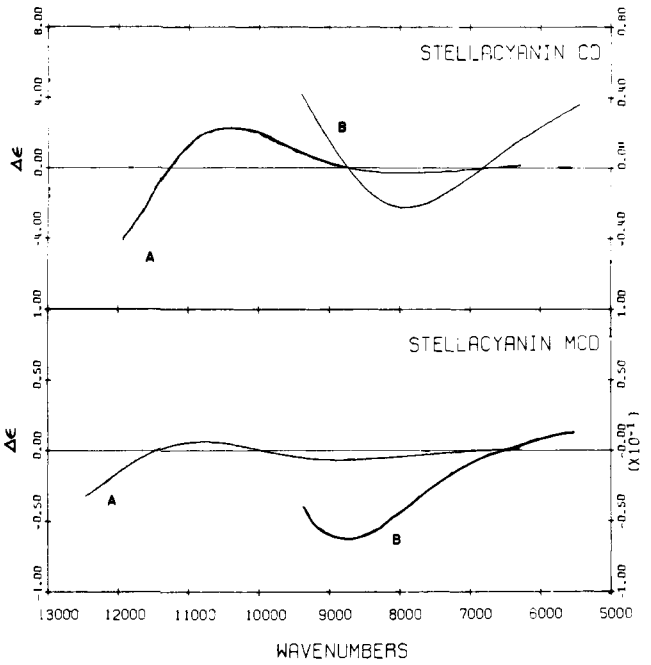

Figure 3. Top frame: the near-infrared CD spectrum of 1.06 mM stellacyanin in a pD 6 deuterated phosphate buffer at 290 K; curve A, left-hand scale; curve B, right-hand scale. Bottom frame: the near-infrared MCD spectrum of 1.06 mM stellacyanin in pD 6 deuterated phosphate buffer at 290 K; curve A, left-hand scale; curve B, right-hand scale.

Table I. Gaussian Analysis of Stellacyanin Absorption Spectra[a]

T = 35 K	60 K	120 K	200 K	270 K
		Band 1		
$\bar{\nu}$ = 22 550	22 570	22 520	22 380	22 210
hwhm = 1185	1196	1265	1457	1512
f = 0.012	0.012	0.012	0.014	0.012
ϵ = 1177	1174	1124	1110	942
		Band 2		
$\bar{\nu}$ = 17 840	17 750	17 630	17 620	17 490
hwhm = 941.5	967	990	1134	1213
f = 0.013	0.015	0.017	0.016	0.016
ϵ = 1631	1769	1927	1658	1542
		Band 3		
$\bar{\nu}$ = 16 460	16 430	16 350	16 310	16 220
hwhm = 883	876	889	1012	1090
f = 0.039	0.037	0.034	0.035	0.033
ϵ = 5046	4879	4371	3995	3549
		Band 4		
$\bar{\nu}$ = 12 510	12 590	12 600	12 680	12 680
hwhm = 867	846	781	863	933
f = 0.0049	0.0039	0.0030	0.0031	0.0027
ϵ = 657	535	445	417	341
		Band 5		
$\bar{\nu}$ = 10 910	11 050	11 060	11 090	11 110
hwhm = 999	1180	1219	1266	1375
f = 0.0053	0.0064	0.0065	0.0066	0.0067
ϵ = 610	627	615	600	565

[a] $\bar{\nu}$ and hwhm in cm^{-1}.

Gaussian resolution of the 35 K spectrum of plastocyanin. The position, intensity, hwhm, and oscillator strength of each of the Gaussian band components in plastocyanin as a function of temperature are set out in Table II.

The visible CD and MCD curves for plastocyanin are shown in Figure 5. The plastocyanin CD spectrum has the same general shape as the stellacyanin CD curve. The main difference in the absorption and CD spectra of stellacyanin and plastocyanin occurs in the activity around 22 500 cm^{-1}. In

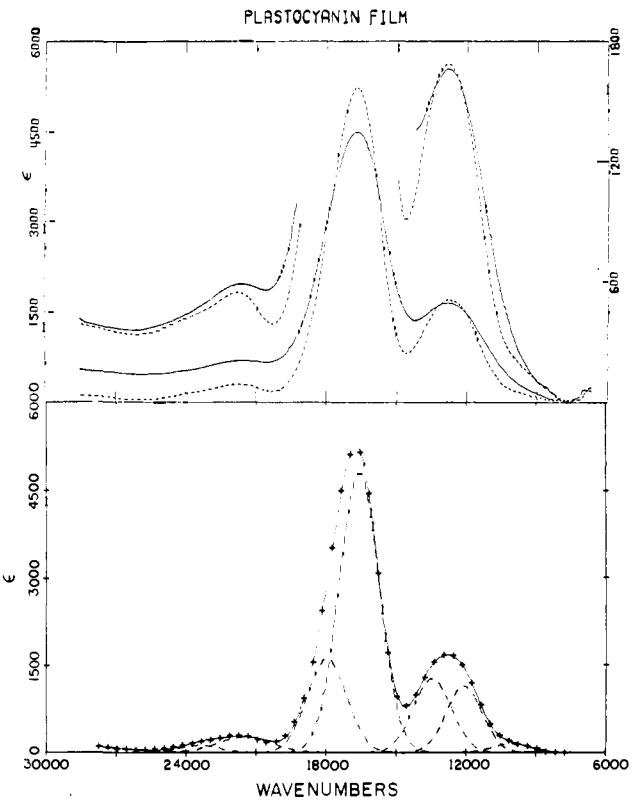

Figure 4. Top frame: the near-infrared and visible absorption spectra of plastocyanin films at 270 (—) and 35 K (---); lower curves, left-hand scale; upper curves (thick film), right-hand scale. Bottom frame: Gaussian resolution of the 35 K near-infrared and visible absorption spectrum of a plastocyanin film; the symbols (+) represent the experimental absorption spectrum.

plastocyanin, two absorption peaks are observed, at 21 800 and 24 000 cm^{-1}, and the CD shows a negative feature at 21 200 cm^{-1} and a positive band at 24 000 cm^{-1}. In this region stellacyanin exhibits only one absorption band and one CD feature, both at 22 500 cm^{-1}.

The MCD spectrum of plastocyanin shows a band at 14 000 cm^{-1}, very weak activity at ~22 500 cm^{-1}, and stronger activity at 36 000 cm^{-1}. No MCD activity attributable to tryptophan is observed in the 34 000-cm^{-1} region, consistent with the amino acid analysis of Milne and Wells.[21] Low-energy CD and MCD curves for plastocyanin are displayed in Figure 6. Near infrared CD bands are clearly evident at 5000, 9150, and 11 200 cm^{-1}. The near-infrared MCD spectrum shows a minimum at 10 600 cm^{-1}.

The absorption spectra of *Pseudomonas aeruginosa* azurin films are shown in Figure 7. The 270 K film spectrum matches the solution spectrum of Tang et al.[22] Narrowing of the 12 400-cm^{-1} band at 35 K reveals a weak absorption at ~10 000 cm^{-1} in the thick film spectrum (B). The resolved Gaussian bands from the 35 K spectrum of azurin are also shown in Figure 7. The Gaussian position, hwhm, and oscillator strength of each component as a function of temperature are listed in Table III.

Our CD spectrum of azurin differs from that reported previously[22] only in that larger negative $\Delta\epsilon$ values are observed in the region below 15 000 cm^{-1} (Figure 8). The visible MCD spectrum of azurin has a negative band at 14 400 cm^{-1}, a weak derivative-like signal centered at 24 300 cm^{-1}, and strong activity associated with tryptophan at ~34 000 cm^{-1} (Figure 8). Bands are resolved at 5800 and ~12 500 cm^{-1} in the near-infrared CD spectrum (Figure 9). No other low-energy bands are prominent, although there is an indication of very weak CD activity at about 10 000 cm^{-1}. It should also be noted

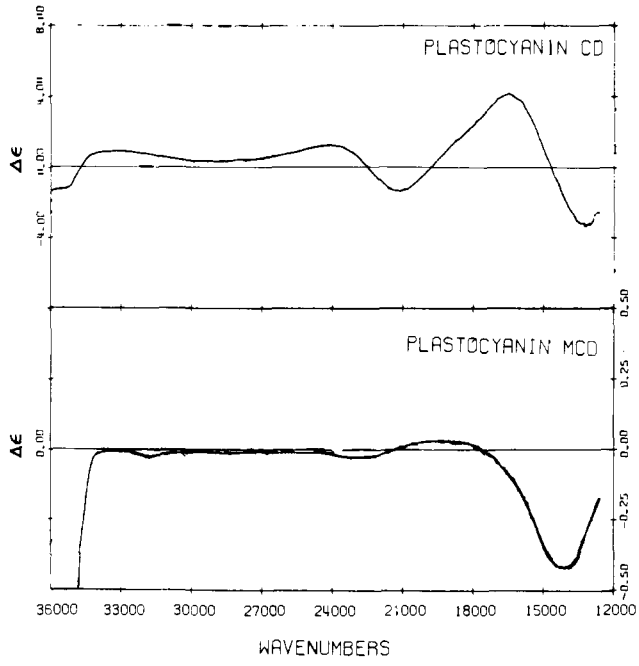

Figure 5. Top frame: the visible CD spectrum of 0.197 mM plastocyanin in pD 6 deuterated phosphate buffer at 290 K. Bottom frame: the visible MCD spectrum of 0.197 mM plastocyanin in deuterated phosphate buffer at 290 K.

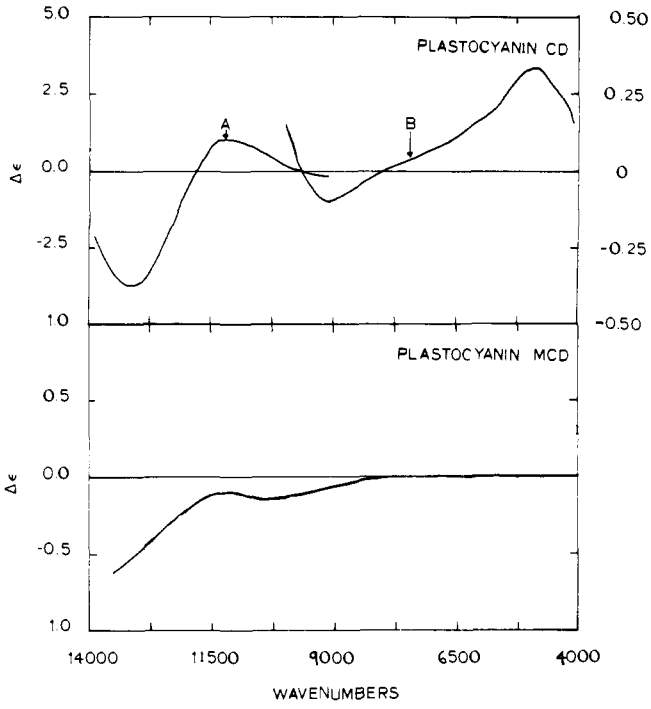

Figure 6. Top frame: the near-infrared CD spectrum of plastocyanin in D_2O at 290 K; curve A, left-hand scale; curve B, right-hand scale. Bottom frame: the near-infrared MCD spectrum of plastocyanin in D_2O solution at 290 K.

that measurements on a reduced azurin sample revealed no CD bands in the near-infrared region. The near-infrared MCD spectrum of azurin exhibits a negative band at ~10 500 cm^{-1} (Figure 9).

Discussion

Theoretical Considerations. The lowest absorption, CD, and MCD features (≤11 500 cm^{-1}) are attributable[3] to d-d transitions in the blue copper centers of the three proteins under study. The positions of these d-d bands ensure that the effective ligand field at the copper site is very weak, which clearly rules out structures based on tetragonal six- and five-coordinate as well as square-planar four-coordinate geometries. Absorption bands at 13 400-14 300 and 17 100-17 500 cm^{-1} attributable to d-d transitions have been reported for several tetragonal CuN_6^{2+} species.[23] The square-pyramidal $Cu(NH_3)_5^{2+}$ ion has d-d electronic transitions at 11 400 and 15 000 cm^{-1}.[23a] The spectra commonly observed[24] for square-planar copper(II)-amino acid complexes show d-d absorption in the ranges 15 400-17 700 and 17 500-20 600 cm^{-1}.[25] Bands at 13 000 and 21 000 cm^{-1} have been observed in the d-d spectrum of a square-planar Cu(II) complex with an N_2S_2 donor set.[26]

Trigonal five- and four-coordinate Cu(II) structures are inconsistent with the known ground-state (EPR) properties of blue copper ($2.0 < g_\perp < g_\parallel$).[2] Typical trigonal bipyramidal copper(II) complexes show a "reversed" ($g_\parallel \simeq 2.0 < g_\perp$) axial EPR spectrum.[27,28] This is the expected ordering for an axially compressed trigonal bipyramid (d_{z^2} ground state for a one-electron hole).[29,30] Even the $Cu(NH_3)_2(NCS)_3^-$ ion, which contains longer axial bond lengths (to ammonia) than equatorial (to isothiocyanate), shows this "reversed" axial spectrum (the higher ligand field strength of ammonia compared to isothiocyanate presumably causes the effective field to be compressed). Expansion along the trigonal axis will eventually result in a ground-state change from $^2A_1(d_{z^2})$ to $^2E'(d_{x^2-y^2}, d_{xy})$, assuming D_{3h} symmetry. Using the distorted trigonal bipyramidal energy matrices of Becker et al.,[31] the energy assignments of Slade et al.,[27] and the equatorial to axial bond length ratio 1.04 reported by Bernal et al.,[32] values of −1425 and −920 cm^{-1} are calculated for the radial parameters[31] *Db*

Table II. Gaussian Analysis of Plastocyanin Absorption Spectra[a]

T = 35 K	60 K	120 K	200 K	270 K
		Band 1		
$\bar{\nu}$ = 23 340				
f = 0.0024				
		Band 2		
$\bar{\nu}$ = 21 390	21 310	22 010	21 910	22 200
hwhm = 1418	1874	2648	2757	2757
f = 0.0035	0.0060	0.011	0.012	0.019
ϵ = 288	370	495	518	811
		Band 3		
$\bar{\nu}$ = 17 870	18 000	18 020	17 880	18 100
hwhm = 985	921	926	1010	1162
f = 0.015	0.014	0.011	0.012	0.012
ϵ = 1719	1736	1314	1402	1163
		Band 4		
$\bar{\nu}$ = 16 490	16 620	16 540	16 440	16 500
hwhm = 1003	980	1063	1148	1301
f = 0.044	0.046	0.049	0.043	0.049
ϵ = 5111	5407	5319	4354	4364
		Band 5		
$\bar{\nu}$ = 13 350	13 390	13 300	13 360	13 330
hwhm = 959	962	966	1027	1108
f = 0.011	0.012	0.011	0.011	0.012
ϵ = 1354	1481	1371	2134	1289
		Band 6		
$\bar{\nu}$ = 11 990	12 080	11 930	11 870	11 810
hwhm = 910	843	910	1043	1125
f = 0.0096	0.0084	0.0089	0.010	0.011
ϵ = 1222	1147	1136	1148	1162
		Band 7		
$\bar{\nu}$ = 9970	10 150	10 000	9820	9530
f = 0.0013	0.0013	0.0013	0.0014	0.0020

[a] $\bar{\nu}$ and hwhm in cm^{-1}.

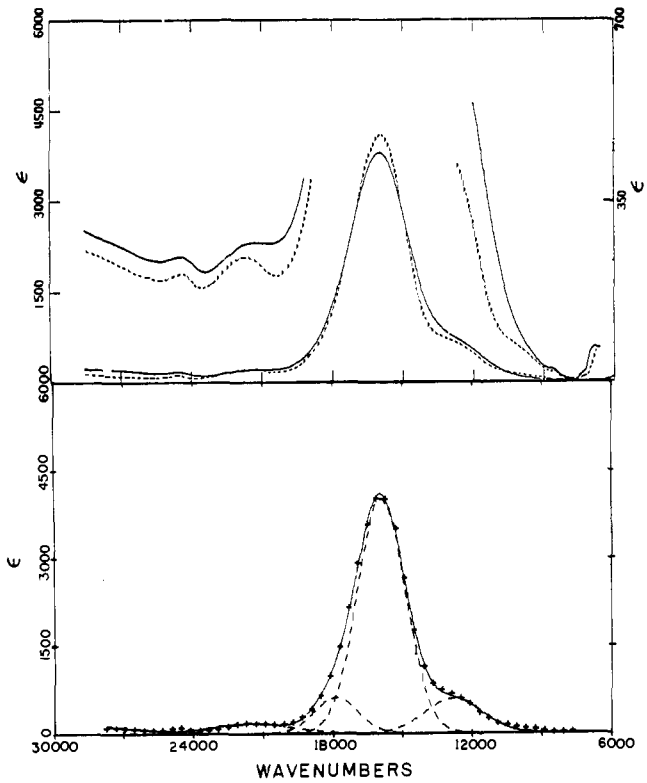

Figure 7. Top frame: the near-infrared and visible absorption spectra of azurin films at 270 (—) and 35 K (---); lower curves, left-hand scale; upper curves (thick film), right-hand scale. Bottom frame: Gaussian resolution of the 35 K near-infrared and visible absorption spectrum of an azurin film; the symbols (+) represent the experimental absorption spectrum.

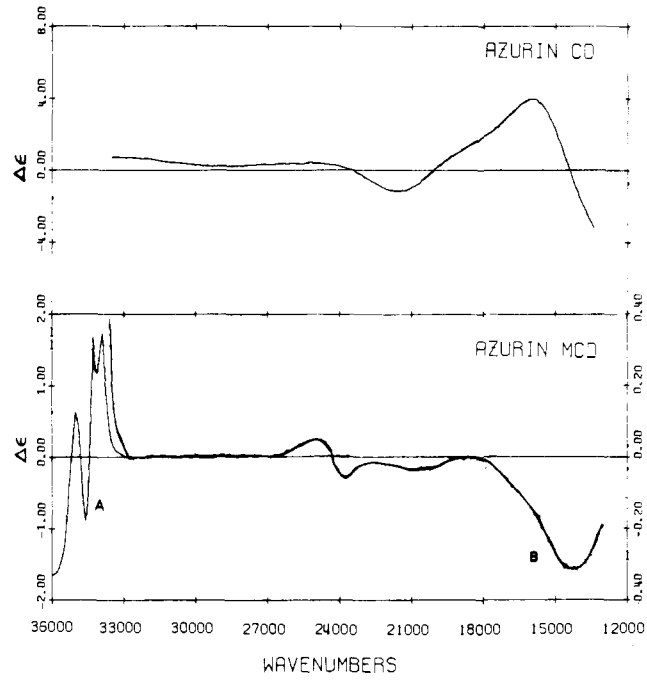

Figure 8. Top frame: the visible CD spectrum of 0.21 mM azurin in pD 6 deuterated phosphate buffer at 290 K. Bottom frame: the visible MCD spectrum of 0.21 mM azurin in pD 6 deuterated phosphate buffer at 290 K; curve A, left-hand scale; curve B, right-hand scale.

and Dq, respectively, for the $CuCl_5^{3-}$ ion. By varying the axial bond length, the $^2E'$ term becomes the ground state at ~2.8 Å. Very long axial distances would be required for the electronic transitions to approach those observed in the blue copper

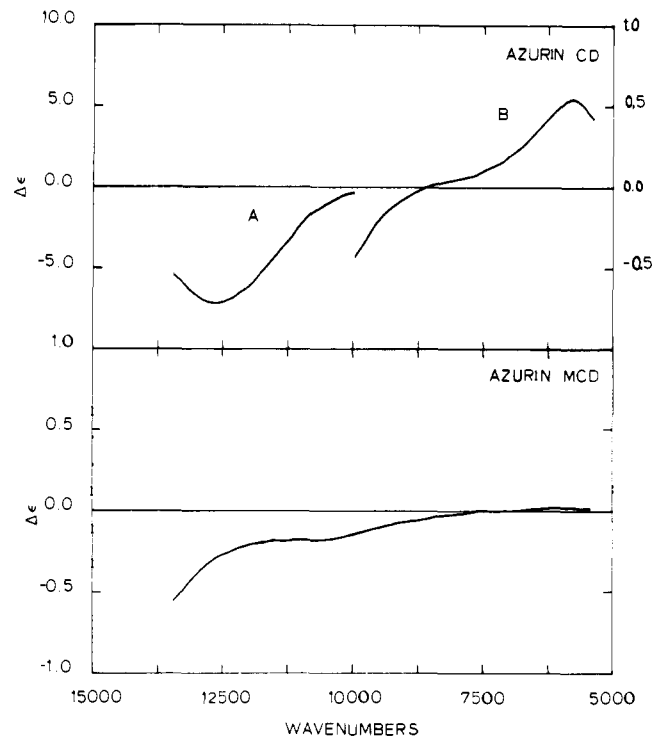

Figure 9. Top frame: the near-infrared CD spectrum of azurin in D_2O solution at 290 K; curve A, left-hand scale; curve B, right-hand scale. Bottom frame: the near-infrared MCD spectrum of azurin in D_2O solution at 290 K.

Table III. Gaussian Analysis of Azurin Absorption Spectra[a]

T = 35 K	60 K	120 K	200 K	270 K
		Band 1		
$\bar{\nu}$ = 21 450	20 060	20 400	21 410	20 790
hwhm = 2099	2090	2984	3680	4144
f = 0.0034	0.0026	0.0026	0.0059	0.0071
ϵ = 185	145	101	185	198
		Band 2		
$\bar{\nu}$ = 17 820	17 600	17 540	17 590	17 650
hwhm = 1078	1038	1099	1156	1252
f = 0.006	0.007	0.0072	0.0064	0.0055
ϵ = 641	778	755	640	504
		Band 3		
$\bar{\nu}$ = 15 870	15 860	15 820	15 810	15 850
hwhm = 1210	1174	1206	1261	1334
f = 0.045	0.042	0.042	0.042	0.044
ϵ = 4278	4167	4021	3826	3798
		Band 4		
$\bar{\nu}$ = 12 770	12 920	12 800	12 810	12 830
hwhm = 1468	1592	1380	1500	1591
f = 0.008	0.0083	0.0067	0.0084	0.0094
ϵ = 632	605	566	647	686

[a] $\bar{\nu}$ and hwhm in cm^{-1}.

proteins. Although it is possible for the protein to constrain ligation around copper(II) to such a coordination (essentially trigonal planar geometry), the predicted g values for such a configuration are different from those observed for the blue copper sites. Spin-orbit coupling splits the $^2E'$ state into $\Gamma_7 + \Gamma_9$ representations of the D_{3h} double group.[31] For a d^9 system Γ_7 becomes the ground state, and there is no excited state of the same symmetry. The calculated g values for this state are $g_\parallel = 2(2k + 1)$ and $g_\perp = 0$, where k is the orbital reduction factor. Thus neither trigonal five-coordinate geometry will yield g values comparable to those observed in the proteins.

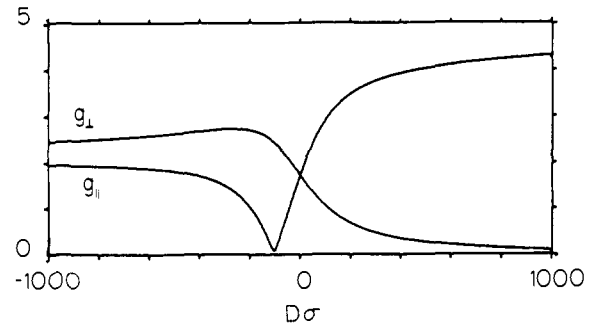

Figure 10. Plot of $g_\parallel$ and $g_\perp$ for $Dq = 500\ cm^{-1}$, $k = 0.6$, and $D\sigma/D\tau = 4$ with $D\sigma$ varying from +1000 to −1000 cm^{-1}.

The compressed trigonal four-coordinate geometry will also have a $^2A_1(d_{z^2})$ ground state for copper(II). Thus, the "inverted" axial EPR spectrum with $g_\parallel \simeq 2.0$ and $g_\perp = 2 - 6k\lambda_0/\Delta$[33] is again expected. This ordering is observed for copper(II) doped into zinc oxide ($g_\parallel = 0.74$ and $g_\perp = 1.53$).[34] (The magnitude of the g values is at variance with the theoretical prediction because the very small trigonal distortion in the zinc oxide site allows configurational interaction between the ground state and a spin-orbit component of $^2E(t_2)$, which has the same double group representation, thereby invalidating the perturbative approximation used[33] to determine the g values.) Expansion along the trigonal axis allows $^2E(t_2)$ to become the ground state. For the large axial distortions necessary to account for the observed protein electronic absorption bands, the g values, using the perturbative method, are calculated to be $g_\parallel = 2(k + 1 - 2\lambda_0(2 + k)/3\Delta_2)$ and $g_\perp = -2k\lambda_0/\Delta_1$, where $\Delta_1 = {}^2A_1 \leftarrow {}^2E(t_2)$, $\Delta_2 = {}^2E(e) \leftarrow {}^2E(t_2)$, and configurational mixing of the $^2E(e)$ excited state with the ground state in the ligand field is ignored.

For the general case where no assumption is made concerning the relative sizes of the ligand field and spin-orbit Hamiltonians, the energy matrices are diagonalized after applying both operators. Since either distortion produces a Γ_4 (C_{3v} double group representation[35]) ground state, only the Γ_4 energy matrix need be diagonalized to predict g values. Using Ballhausen's trigonal basis set ($\{t_2^a, t_2^b\} = E$, $t_2^0 = A_1$, $\{e^a, e^b\} = E$ in C_{3v}) and trigonal ligand field operator,[33] the energy matrix shown in eq 1 is obtained.

$$\begin{vmatrix} \underline{(-t_2^b\beta)} & \underline{(t_2^0\alpha)} & \underline{(-e^b\beta)} \\ -D\sigma - \tfrac{2}{3}D\tau - 4Dq + (\lambda/2) - E & -\frac{\sqrt{2}}{2}\lambda & -\sqrt{2}D\sigma + (5\sqrt{2}/3)D\tau + \frac{\sqrt{2}}{2}\lambda \\ -\frac{\sqrt{2}}{2}\lambda & 2D\sigma + 6D\tau - 4Dq - E & \lambda \\ -\sqrt{2}D\sigma + (5\sqrt{2}/3)D\tau + \frac{\sqrt{2}}{2}\lambda & \lambda & (-7/3)D\tau + 6Dq - E \end{vmatrix} = 0 \quad (1)$$

This matrix is similar to that of Liehr,[36] who diagonalizes the trigonal basis set in the T_d double group before adding the trigonal field and spin-orbit coupling. The ground-state wave function is therefore $\Psi_{\Gamma_4}{}^{gs} = a(-t_2^b\beta) + b(t_2^0\alpha) + c(-e^b\beta)$, where the coefficients a, b, and c are determined by diagonalization of the energy matrix. The g values can be written in terms of these coefficients as follows:

$$\begin{aligned} g_\parallel &= 2[(-1 - k)a^2 + b^2 - 2\sqrt{2}kac] \\ g_\perp &= 2[b^2 - \sqrt{2}kab + 2kbc] \end{aligned} \quad (2)$$

where k is the orbital reduction factor. A plot of $g_\parallel$ and $g_\perp$ for a Dq value of 500 cm^{-1}, an orbital reduction factor of 0.6, a $D\sigma$ to $D\tau$ ratio of 4, and variation of $D\sigma$ from +1000 to −1000 cm^{-1} is shown in Figure 10. The unusual shape of $g_\parallel$ arises from the spin-orbit Hamiltonian mixing $t_2^0\alpha$ with $(-t_2^b)\beta$. As the g value is defined by the equation $g_i\beta H_z = \langle\Psi^{gs}\alpha|\mu_z|\Psi^{gs}\alpha\rangle - \langle\Psi^{gs}\beta|\mu_z|\Psi^{gs}\beta$, where μ_z is the z component of the Zeeman operator, the value is positive when $b > a$ ($t_2^0\alpha$ is the ground state) and negative when $a > b$ ($(-t_2^b)\beta$ is the ground state). The EPR experiment, of course, measures only the magnitude of g. The values of $g_\parallel$ and $g_\perp$ do not cross at 2 (the limit of zero axial field) as the orbital reduction factor was also included in the spin-orbit operator, $\lambda(kl)s$, yielding an isotropic value of $2.00(k)$. It is apparent from inspection of Figure 10 that the g values of blue copper ($g_\parallel \simeq 2.25$, $g_\perp \simeq 2.05$)[2] cannot be accommodated by a trigonally distorted structure.[37,38]

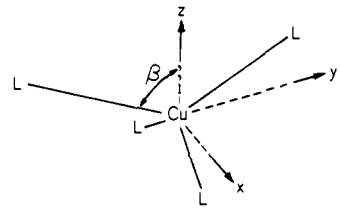

Figure 11. Reference coordinate system for the flattened tetrahedral (D_{2d}) ligand field model.

A tetragonally flattened tetrahedral Cu(II) geometry is consistent with the EPR parameters of blue copper, as in this case we have

$$g_\parallel = 2 - \frac{8k\lambda_0}{\Delta_2} \text{ and } g_\perp = 2 - \frac{2k\lambda_0}{\Delta_3} \quad (3)$$

where $\Delta_2 = {}^2B_1 \leftarrow {}^2B_2$ and $\Delta_3 = {}^2E \leftarrow {}^2B_2$.[33] For facile correlation with the square-planar limit, we have chosen a coordinate system (Figure 11) in which the tetrahedral t_2 orbital set is $\{(xz), (yz), (x^2 - y^2)\}$. In this system a tetragonal distortion toward the square-planar configuration would be expected to yield a $^2B_2(d_{x^2-y^2})$ ground state for Cu(II). The extent of this distortion is given by the angle β, as defined in Figure 11. The ligand field potential should, therefore, retain this angle as a variable, along with the usual radial integrals. The D_{2d} potential has the following form:

$$V = \gamma_2{}^0[3z^2 - r^2] + \gamma_4{}^0[35z^4 - 30z^2r^2 + 3r^4] + \gamma_4{}^4[x^4 - 6x^2y^2 + y^4] \quad (4)$$

where $\gamma_n{}^m = [4\pi ze/(2n + 1)a^{n+1}]\Sigma_i Y_n{}^m(r_i, \theta_i, \phi_i)$ and $Y_n{}^m(r_i, \theta_i, \phi_i)$ is a spherical harmonic. Evaluation of the spherical harmonics for ligands at $(a, \beta, 0)$, (a, β, π), $(a, 180 - \beta, \pi/2)$, and $(a, 180 - \beta, 3\pi/2)$ yields

$$V = ze(3\cos^2\beta - 1)]3z^2 - r^2]/a^3 + ze(35\cos^4\beta - 30\cos^2\beta + 3)[35z^4 - 30z^2r^2 + 3r^4]16a^5 + ze(35\sin^4\beta)[x^4 - 6x^2y^2 + y^4]/16a^5 \quad (5)$$

The values of the one-electron energies may be obtained by direct integration using this form of the potential. Our procedure, however, employed an operator equivalent form, which saves a great deal of computation. The operator equivalent

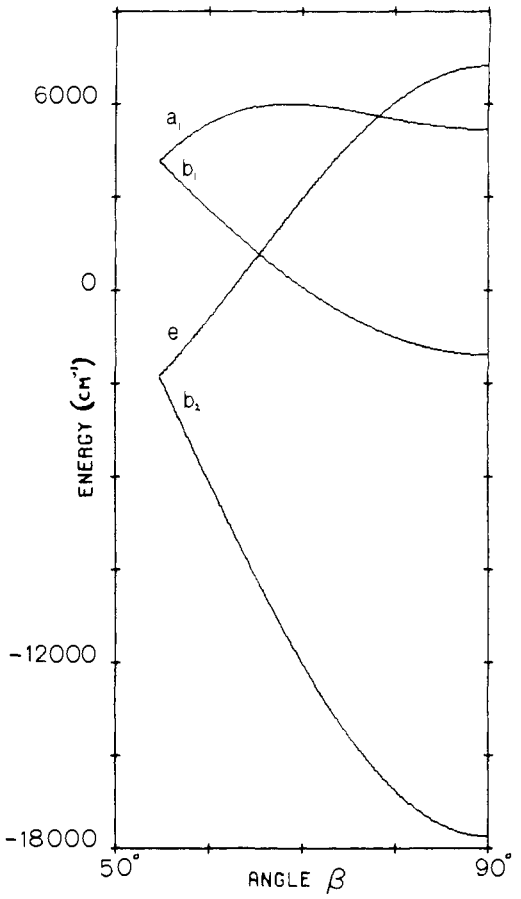

Figure 12. The angular dependences of the b_2 ($d_{x^2-y^2}$), e (d_{xz}, d_{yz}), b_1 (d_{xy}), and a_1 (d_{z^2}) hole energies as a function of β for a d^9 ion (Ds = 765 cm^{-1}, Dt = 444 cm^{-1}).

expression for D_{2d} symmetry is as follows:

$$V = ze\alpha_2(3\cos^2\beta - 1)[3\hat{l}_z^2 - \hat{l}^2]\langle r^2\rangle/a^3 + ze\alpha_4(35\cos^4\beta - 30\cos^2\beta + 3) \times [35\hat{l}_z^4 - 30\hat{l}^2\hat{l}_z^2 + 25\hat{l}_z^2 - 6\hat{l}^2 + 3(\hat{l}^2)^2]\langle r^4\rangle/16a^5 + 35ze\alpha_4\sin^4\beta[\hat{l}_+^4 + \hat{l}_-^4]\langle r^4\rangle/32a^5 \quad (6)$$

where $\alpha_2 = 2/21$, $\alpha_4 = -2/63$, and $\langle r^n\rangle$ is the radial integral $\int r^{n+2}R^2_{(n,l)}dr$. The d electron hole energies are calculated to be

$$W(a_1 = d_{z^2}) = -12(3\cos^2\beta - 1)Ds - 3\delta Dt$$
$$W(b_1 = d_{xy}) = 12(3\cos^2\beta - 1)Ds + \tfrac{1}{2}(35\sin^4\beta - \delta)Dt$$
$$W(e = d_{xz}, d_{yz}) = -6(3\cos^2\beta - 1)Ds + 2\delta Dt$$
$$W(b_2 = d_{x^2-y^2}) = 12(3\cos^2\beta - 1)Ds - \tfrac{1}{2}(35\sin^4\beta + \delta)Dt \quad (7)$$

where $\delta = 35\cos^4\beta - 30\cos^2\beta + 3$, $Ds = ze\langle r^2\rangle/21a^3$, and $Dt = ze\langle r^4\rangle/21a^5$. These energy levels are plotted as a function of β (the distortion angle) in Figure 12.

Model Systems. We have tested the β-parametrized D_{2d} ligand field model on a series of tetrachlorocuprates of varying (β = 64-90°) structures. The procedure involved variation of the radial parameters and the distortion angle β to obtain a best fit with the observed d-d energies and the square-planar limit. In all four flattened tetrahedral $CuCl_4^{2-}$ complexes the calculated β is within 2° of the experimental value (Table IV). Our calculations compare favorably to similar work[39-44] but the derived radial parameters are somewhat better because a larger set of chlorocuprates has been considered and $Pt(NH_3)_4CuCl_4$ has been replaced by bis(*N*-methylphenethylammonium)tetrachlorocuprate(II) as the square planar limit (the structure of the former compound shows that the copper experiences significant axial interactions with neighboring ions; such interactions are absent in the latter complex).[44] The important point to make here is that a reasonable estimate of the distortion in a D_{2d} $CuCl_4^{2-}$ complex may be obtained from an analysis of its d-d spectrum. We have not included spin-orbit coupling in the calculations, as such effects do not change the predicted β values in the region of interest ($\beta \geq 60°$).

Systematic changes in the absorption and EPR spectra and redox potentials of a series of pyrrole-2-carboxaldehyde Schiff base copper(II) complexes[45] effected by decreasing the dihedral angle 2ω between the chelate ring planes by varying the bulkiness of the ligand side groups are also consistent with the ligand field model. An earlier series of nitrogen-ligated copper(II) complexes of D_2 symmetry was also characterized in terms of the dihedral angle 2ω by Marakami et al.,[46] who showed the relation to the distortion angle β to be $\cos\beta = \sin\alpha \sin\omega$, where 2α is the N-Cu-N angle within one of the chelate rings. The EPR spectra of a limited series of CuS_4 complexes are also predictable in terms of the above ligand field.[47] In view of all the electronic spectral and EPR results discussed in this and the previous section, we eye with suspicion statements[48] to the effect that a distortion from square-planar geometry is not a prerequisite for explaining the observed physical properties of blue copper centers.

Blue Copper Ligand Fields. For β values near the tetrahedral limit the order of excited states is $^2E < {}^2B_1 < {}^2A_1$. Calculations on plastocyanin show that only β's near 60° can fit the three transitions and at the same time give reasonable energies for the square-planar limit. Taking $\Delta W(^2E_2 - {}^2B_2) = 5000$ cm^{-1} and $\Delta W(^2B_1 - B_2) = 9150$ cm^{-1}, the procedure is to calculate $\Delta W(^2A_1 - {}^2B_2)$ for various values of β near 60°. For β = 62°, Ds = 407 cm^{-1}, Dt = 430 cm^{-1}, $\Delta W(^2A_1 - {}^2B_2)$ is calculated to be 9938 cm^{-1} ($\Delta W(^2A_{1g} - {}^2B_{1g})$, the D_{4h} limit, is calculated to be 14 066 cm^{-1}); for β = 58°, Ds = 1337 cm^{-1}, Dt = 505 cm^{-1}, $\Delta W(^2A_1 - {}^2B_2)$ = 12 991 cm^{-1}, D_{4h} limit = 37 135 cm^{-1}; for β = 60°, Ds = 691 cm^{-1}, Dt = 465 cm^{-1}, $\Delta W(^2A_1 - {}^2B_2)$ = 11 412 cm^{-1}, D_{4h} limit = 21 200 cm^{-1}. Since the observed $^2A_1 \rightarrow {}^2B_2$ transition falls between 11 200 (CD) and 11 810 cm^{-1} (absorption), β = 60° is to be preferred. Furthermore, the β = 58 and 62° calculations give unreasonably high and low D_{4h} limits, respectively, for a $Cu^{II}N_2S_2$ complex. The 11 810-cm^{-1} absorption band is several times more intense than the 9150-cm^{-1} band (Table V), consistent with D_{2d} selection rules: $^2B_2 \rightarrow {}^2A_1$ is electric dipole allowed but $^2B_2 \rightarrow {}^2B_1$ is forbidden.

Complete d-d band assignments and ligand field parameters for the three blue proteins are summarized in Table V. For all three blue copper centers the β values fall in the narrow range 60-61°, providing additional evidence of the close similarities in coordination structure. The ligand field parameters are not as well determined for azurin and stellacyanin as they are for plastocyanin, as in the former two cases there are larger uncertainties in the positions of the d-d transitions.

The EPR spectrum of plastocyanin has been fit by an axial spin Hamiltonian with the values $\lambda_0 = -828$ cm^{-1}, $g_\parallel = 2.226$, and $g_\perp = 2.053$.[20] Using eq 3, values of $k_\parallel$ and $k_\perp$ are computed to be 0.31 and 0.16, respectively. These values are much lower than those calculated for square-planar copper-peptide complexes, where $k_\parallel$ falls in the range 0.64-0.55 and $k_\perp$ between 0.71 and 0.45.[25] Using the orbital reduction factors calculated for plastocyanin and the observed energy splittings for azurin and stellacyanin, $g_\parallel = 2.20$, $g_\perp = 2.05$, and $g_\parallel = 2.18$, $g_\perp = 2.05$[49] are predicted for azurin and stellacyanin, respectively. Observed values are $g_\parallel = 2.260$, $g_\perp = 2.052$ for azurin[50] and $g_z = 2.287$, $g_y = 2.077$, $g_x = 2.025$ for stellacyanin.[51] Unusually low hyperfine coupling constants are

Table IV. Structural and Electronic Spectroscopic Data and Calculated Ligand Field Parameters for Tetrachlorocuprates

counterion	R(Cu-Cl) (av), Å	β(av), deg	$\bar{\nu}$(obsd), cm^{-1}	$\bar{\nu}$(calcd), cm^{-1}	β(calcd), deg	Ds, cm^{-1} [a]	Dt, cm^{-1}
Cs^+	2.23	65[b]	5 175[c]	5 193	63	415	345
			7 900	7 610			
			9 050	9 070			
Me_3BzN^+	2.27	66[d]	5 920[d]	5 514	64	415	345
				7 746			
			9 200	9 251			
$Me_2H_2N^+$	2.23	68[e]	5 750[f]	7 937	68	400	350
			9 200	8 925			
			10 300	10 407			
Ph_4As^+	2.26	73[g]	8 930[g]	9 266	73	445	320
				10 929			
			12 200	11 957			

[a] Each set of Ds and Dt values gives an acceptable fit to the D_{4h} $CuCl_4^{2-}$ spectrum; experimental band positions for the *N*-methylphenethylammonium salt of $CuCl_4^{2-}$ ($\beta = 90°$, R(Cu-Cl) = 2.27 Å) are 11 500, 13 600, and 16 100 cm^{-1} (R. L. Harlow, W. J. Wells III, G. W. Watt, and S. H. Simonsen, *Inorg. Chem.*, **13**, 2106 (1974)); the D_{4h} spectrum is fit exactly by Ds = 431 and Dt = 334 cm^{-1}. [b] J. A. McGinnety, *J. Am. Chem. Soc.*, **94**, 8406 (1972). [c] J. Ferguson, *J. Chem. Phys.*, **40**, 3406 (1964). [d] C. Furlani, E. Cervone, F. Calzona, and B. Baldanza, *Theor. Chim. Acta*, **7**, 375 (1967). [e] R. D. Willett and M. L. Larsen, *Inorg. Chim. Acta*, **5**, 175 (1971). [f] R. D. Willett, J. A. Haugen, J. Lesback, and J. Morrey, *Inorg. Chem.*, **13**, 2510 (1974). [g] Analysis is for the $[CuCl_4]$ fragment in $Cu_2Cl_6^{2-}$; R. D. Willett and C. Chow, *Acta Crystallogr., Sect. B*, **30**, 207 (1974).

Table V. d-d Bands and Ligand Field Parameters for Plastocyanin, Azurin, and Stellacyanin

LF parameters	absorption (270 K) $\bar{\nu}$, cm^{-1}	absorption (270 K) ϵ	CD (295 K) $\bar{\nu}$, cm^{-1}	CD (295 K) $\Delta\epsilon$	MCD (295 K) $\bar{\nu}$, cm^{-1}	MCD (295 K) $\Delta\epsilon$	γ	assignment
			Plastocyanin					
$\beta = 60°$	*a*	~100	5000	0.35			0.0035	$^2B_2 \rightarrow {}^2E$
Ds = 691 cm^{-1}	9350	200	9150	−0.10			0.0005	$^2B_2 \rightarrow {}^2B_1$
Dt = 465 cm^{-1}	11 810	1162	11 200	1.1	10 600	−0.15	0.0009	$^2B_2 \rightarrow {}^2A_1$
D_{4h} limit = 21 330 cm^{-1}	(11 400)[b]							
			Azurin					
$\beta = 61°$	*a*	~100	5800	0.54			0.0054	$^2B_2 \rightarrow {}^2E$
Ds = 700 cm^{-1}	~10 000[a]	~125	10 200	−0.20	10 500	−0.18	0.0016	$^2B_2 \rightarrow {}^2B_1$
Dt = 480 cm^{-1}	(12 410)[b]							$^2B_2 \rightarrow {}^2A_1$
D_{4h} limit = 21 600 cm^{-1}								
			Stellacyanin[c]					
$\beta = 60°$	*a*	~100	5250	0.45			0.0045	$^2B_2 \rightarrow {}^2E$
Ds = 765 cm^{-1}	8800[a]	~100	8100	−0.35	8800	−0.08	0.0035	$^2B_2 \rightarrow {}^2B_1$
Dt = 444 cm^{-1}	11 110	565	10 500	2.4	10 800	+0.08	0.0042	$^2B_2 \rightarrow {}^2A_1$
D_{4h} limit = 22 800 cm^{-1}	(11 500)[b]							

[a] Not resolved at 270 K; band positions and ϵ's are estimated from the 35 K absorption spectrum. [b] Calculated position of $^2B_2 \rightarrow {}^2A_1$. [c] Parameters are for the fit to 5250- and 8800-cm^{-1} transition energies; an equally acceptable fit to these energies is obtained for $\beta = 61°$ (Ds = 588, Dt = 430, D_{4h} limit = 18 416 cm^{-1}), with $^2B_2 \rightarrow {}^2A_1$ at 10 843 cm^{-1}. Alternatively, a fit to 5250 and 8100 cm^{-1} for $\beta = 61°$ (Ds = 620, Dt = 395, D_{4h} limit = 18 849 cm^{-1}) gives $^2B_2 \rightarrow {}^2A_1$ at 10 526 cm^{-1}.

another spectroscopic characteristic of the blue site. Using the observed g values and the theoretical expressions derived by Bates et al.,[52] values of $A_\parallel$ and $A_\perp$ for stellacyanin, azurin, and plastocyanin were obtained: plastocyanin, $A_\parallel$(calcd) = 0.0115, $A_\parallel$(obsd)[20] = 0.0063, $A_\perp$(calcd) = 0.011, $A_\perp$(obsd)[20] < 0.0017 cm^{-1}; azurin, $A_\parallel$(calcd) = 0.0112, $A_\parallel$(obsd)[50] = 0.006, $A_\perp$(calcd) = 0.0016, $A_\perp$(obsd)[50] ~ 0 cm^{-1}; stellacyanin, A_z(calcd) = 0.0083, A_z(obsd)[51] = 0.0035, A_x(calcd) = 0.0013, A_x(obsd)[51] = 0.0029, A_y(calcd) = 0.0053, A_y(obsd)[51] = 0.0057 cm^{-1}.

The effect of differing radial integral values for nitrogen and sulfur ligands on the energy levels and g values predicted by the tetragonal field was also investigated, using a C_{2v} geometry such that the twofold rotation axis remained along the tetragonal z axis. The energies of the electron hole in this field are identical with those given above for the D_{2d} field if the average of the nitrogen and sulfur radial parameters is substituted for Ds and Dt. In addition, the d_{xz} and d_{yz} levels are split by $18 \sin^2\beta(Ds^N - Ds^S) + 10 \sin^2\beta(7\cos^2\beta - 1)(Dt^N - Dt^S)$ and d_{z^2} mixes with the ground state $d_{x^2-y^2}$. Using the values of β, Ds, and Dt obtained for stellacyanin, and adjusting the ratio Dt^N/Dt^S to be 1.55, the splitting of the d_{xz}, d_{yz} pair is calculated to be 3540 cm^{-1}, consistent with the splitting calculated previously[49] from the experimental g values of stellacyanin.[51]

Reduction Potentials. The reduction potentials of stellacyanin, azurin, and plastocyanin are 184, 330, and 347 mV, respectively.[53] Perhaps the most important point to make is that the ligand field model with $\beta \sim 60°$ (Figure 12) accounts in part for the fact that the blue protein potentials are more positive than that of the tetragonal copper(II) aquo ion (153 mV), owing to the very low theoretical ligand field stabilization energies (LFSE) associated with the tetrahedral site.[8d] The LFSE for stellacyanin is only −6152 cm^{-1} (−4144 cm^{-1} attributable to the tetrahedral field and −2008 cm^{-1} to the tetragonal distortion). For plastocyanin it is −6113 cm^{-1} and for azurin it is −6885 cm^{-1}. The LFSE difference between plastocyanin and aqueous copper(II) is 345 mV (Cu(II) aquo is −8900 cm^{-1}).[8d] Thus, a value of 498 mV is predicted for the reduction potential of plastocyanin. Azurin is destabilized by 250 mV relative to hexaaquocopper(II), which yields a potential of 403 mV. Stellacyanin is destabilized by 340 mV with

Table VI. Charge-Transfer Spectral Data for Plastocyanin, Azurin, and Stellacyanin

protein	absorption[a] $\bar{\nu}$, cm^{-1}	nm	ϵ	CD (295 K) $\bar{\nu}$, cm^{-1}	nm	$\Delta\epsilon$	γ	assignment
plastocyanin	13 330	752	1289	12 800	781	3.78	0.0029	$\pi S \rightarrow d_{x^2-y^2}$
	16 500	606	4364	16 500	606	4.08	0.000 93	$\sigma S \rightarrow d_{x^2-y^2}$
	18 100	552	1163	19 000	526	0.4	0.000 34	$\sigma S^* \rightarrow d_{x^2-y^2}$
	22 200[b]	450	300	21 200	472	−1.32	0.0044	$\pi N \rightarrow d_{x^2-y^2}$
	23 340[b]	428	~100	24 000	417	1.26	0.013	$\pi N \rightarrow d_{x^2-y^2}$
azurin	12 830	779	686	12 500	800	−5.9	0.0086	$\pi S \rightarrow d_{x^2-y^2}$
	15 850	631	3798	16 100	621	6.5	0.0017	$\sigma S \rightarrow d_{x^2-y^2}$
	17 650	567	504	19 000	526	1.2	0.0024	$\sigma S^* \rightarrow d_{x^2-y^2}$
	20 790	481	198	21 400	467	−1.8	0.0091	$\pi N \rightarrow d_{x^2-y^2}$
stellacyanin	12 680	789	341	12 800	781	−5.0	0.015	$\pi S \rightarrow d_{x^2-y^2}$
	16 220	617	3549	16 500	606	3.6	0.0010	$\sigma S \rightarrow d_{x^2-y^2}$
	17 490	676	1542	19 000	526	0.75	0.000 49	*c*
	22 210	450	942	22 400	446	−7.35	0.0078	*c*

[a] Positions and ϵ's for the proteins were taken from Gaussian analyses at 270 K except where noted. [b] Positions and ϵ's were taken from a Gaussian analysis at 35 K. [c] See text.

Table VII. Temperature Dependence of the Bandwidth of the 600-nm Absorption in Blue Proteins

Stellacyanin

band 2			band 3		
T, K	hwhm(calcd)[a]	hwhm(obsd)	*T*, K	hwhm(calcd)[b]	hwhm(obsd)
200	1171	1134	200	994	1012
120	1036	990	120	905	889
60	984	967	60	877	876
35	981	942	35	876	883

Plastocyanin

band 3			band 4		
T, K	hwhm(calcd)[c]	hwhm(obsd)	*T*, K	hwhm(calcd)[d]	hwhm(obsd)
200	1056	1010	200	1171	1148
120	954	926	120	1036	1063
60	922	921	60	984	980
35	921	985	35	981	1003

Azurin

band 2			band 3		
T, K	hwhm (calcd)[e]	hwhm(obsd)	*T*, K	hwhm(calcd)[f]	hwhm(obsd)
200	1151	1156	200	1249	1261
120	1062	1099	120	1185	1206
60	1039	1038	60	1174	1174
35	1038	1078	35	1174	1210

[a] $h\nu = 282 \pm 80\ cm^{-1}$, $c'^2 = 5.88$. [b] $h\nu = 288 \pm 80\ cm^{-1}$, $c'^2 = 4.63$. [c] $h\nu = 277 \pm 70\ cm^{-1}$, $c'^2 = 5.52$. [d] $h\nu = 242 \pm 60\ cm^{-1}$, $c'^2 = 8.21$. [e] $h\nu = 317 \pm 97\ cm^{-1}$, $c'^2 = 5.40$. [f] $h\nu = 387 \pm 147\ cm^{-1}$, $c'^2 = 4.60$.

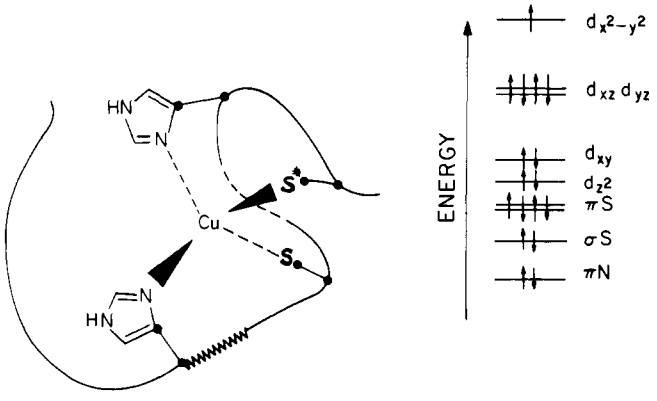

Figure 13. Structural representation of the near-tetrahedral CuN_2SS^* (S = Cys-S; S* = Met-S) center in plastocyanin or azurin. The relative energies of the copper d and selected ligand σ and π orbitals are based on the electronic spectroscopic results (the energy of σS^* is not shown, but is assumed to be approximately equal to σS).

respect to the aquo ion, and its reduction potential is therefore predicted to be 493 mV. Clearly, the loss of LFSE associated with the approximately tetrahedral copper site makes an important contribution to the reduction potential; however, solvation and other environmental effects (possibly related to ligand variation in stellacyanin) are expected to make important contributions to the potentials of blue copper proteins.

Charge-Transfer Transitions. Spectroscopic data for the charge-transfer transitions in plastocyanin, azurin, and stellacyanin are collected in Table VI. The assignments given for the charge-transfer transitions are based on the energy level diagram shown in Figure 13. It is generally accepted that the absorption bands at 13 000 and 16 000 cm^{-1} represent $\pi S \rightarrow$ and $\sigma S \rightarrow Cu(d_{x^2-y^2})$ transitions, respectively.[3] The $\pi S \rightarrow d_{x^2-y^2}$ transition is both electric and magnetic dipole allowed and thus should have a large Kuhn anisotropy factor ($\gamma = |\Delta\epsilon/\epsilon|$),[54] as observed. The $\sigma S \rightarrow d_{x^2-y^2}$ transition is only electric dipole allowed, which is consistent with the relatively low value of γ for the intense absorption band. Strong support for the πS and σS assignments has come from recent studies

of the charge-transfer spectra of several copper(II) complexes containing sulfur-donor ligands.[55,56]

The interpretation of the relatively weak charge-transfer bands that fall above the main blue copper absorption at 16 000 cm^{-1} is in doubt. It is reasonable to expect that a charge-transfer transition originating in the methionine σ-donor sulfur orbital (plastocyanin or azurin) should give rise to a moderately intense ($\epsilon \sim 10^3$) band at about the same energy as the $\sigma S(Cys) \rightarrow Cu(d_{x^2-y^2})$ transition.[55-57] The Kuhn anisotropy factor for this type of transition should again be small, suggesting that the best candidate is the high-energy shoulder (~18 000 cm^{-1}) on the blue band. The bands in the 21 000-23 000-cm^{-1} region in plastocyanin and azurin have large Kuhn anisotropy factors and in each case are tentatively associated with one or more transitions originating in the highest occupied π orbitals of imidazole ($\pi N \rightarrow d_{x^2-y^2}$).

The fact that the electronic spectrum of stellacyanin exhibits a charge-transfer band near 18 000 cm^{-1} indicates that a sulfur donor ligand in addition to cysteine is present at the blue site. Disulfide coordination is particularly attractive, as the ligand field strength it would contribute is quite similar to that of methionine sulfur (recall that nearly equal ligand field transition energies are observed for stellacyanin and plastocyanin). Coordination by disulfide at the stellacyanin blue site is also consistent with the results of recent resonance Raman experiments.[58]

The main features in the visible MCD spectra of the three native proteins (Figures 2, 5, and 8) are similar[59] except in the 16 500-cm^{-1} region, where the stellacyanin spectrum shows significant activity. This is consistent with the presence of new absorption features in the visible region of stellacyanin associated with the required replacement of methionine, and may serve as a reporter of ligand variation in other blue copper proteins. The near-infrared MCD spectrum of stellacyanin is also significantly different from that of plastocyanin or azurin.

It is disappointing that the charge-transfer bands in stellacyanin, plastocyanin, and azurin remain broad and featureless at low temperatures. Given this situation, we have performed moment analysis in order to extract some information concerning vibronic coupling in the excited state. The nth moment is defined as

$$M^n = \int(\nu - \bar{\nu})^n I(\nu)d\nu / \int I(\nu)d\nu \qquad (8)$$

where $\bar{\nu}$ is the mean frequency of the band and $I(\nu)$ is the intensity at ν. Lax has shown[60] that the second moment can be related to the vibrational frequency of a single mode strongly coupled to the electronic wave function (or the mean of many weakly coupled modes), as in the equation

$$M^2 = C^2(h\nu)^2 \coth(h\nu/2kT) \qquad (9)$$

Numerical integration according to eq 8 is the most direct method of obtaining the desired moment, provided that the absorption band is attributable to a single electronic transition. The results for the 16 000-cm^{-1} absorption are given in Tables I, II, and III for stellacyanin, plastocyanin, and azurin, respectively. The second moment of a Gaussian band is easily found to be $(hwhm)^2/2 \ln 2$, so that the half-width at half-maximum can be related to temperature according to the equation

$$(hwhm)^2 = 2C'^2(h\nu^2) \coth(h\nu/2kT) \qquad (10)$$

The values of C'^2 and ν are set out in Table VII. The frequency of the vibrational mode coupled to the σ charge transfer transition varies from 242 ± 60 cm^{-1} for plastocyanin to 387 ± 145 cm^{-1} for azurin. As an elongation of the Cu-S bond must be the dominant distortion in the $\sigma S \rightarrow d_{x^2-y^2}$ excited state, these values provide rough estimates of the effective Cu-S stretching frequencies in these proteins. While the error in this approach is rather large owing to overlapping bands, these numbers are in the correct range of the vibrational frequencies observed[58,61,62] in the resonance Raman spectra obtained on excitation in the 600-nm region. We would expect the Cu-S stretch to be most resonance enhanced by the $\sigma S \rightarrow$ Cu transition and prefer its assignment as one of the intense vibrations in the 390-410-cm^{-1} region. Such an assignment has also been proposed by Woodruff and co-workers based on their resonance Raman studies of stellacyanin and certain Cu-S model complexes.[58]

Concluding Remarks

A great deal of information about the structural nature of blue copper centers has been derived from analysis of electronic spectra. The near-tetrahedral Cu(II) structure nicely accounts for the observation that relatively exposed blue copper sites (e.g., stellacyanin) accept electrons rapidly in reactions with various reagents, as the inner sphere reorganization barrier

$$\text{tetrahedral Cu(II)} \underset{-e^-}{\overset{+e^-}{\rightleftharpoons}} \text{Cu(I)}$$

should be small.[63,64] Whether the ligand binding site constrains the Cu(II) to be nearly tetrahedral by itself or requires some energetic assistance from internal protein interactions is a question deserving further study.

Acknowledgment. We thank Roy Clark for assistance with the near-infrared CD measurements. This research was supported by the National Science Foundation (CHE77-11389). Research at the University of Southern California (P.J.S.) was supported by the National Institutes of Health.

References and Notes

(1) (a) Department of Chemistry, Massachusetts Institute of Technology, Cambridge, Mass. 92139. (b) Department of Chemistry, University of Southern California, Los Angeles, Calif. 90007.
(2) (a) Malkin, R.; Malmström, B. G.; *Adv. Enzymol.* **1970**, *33*, 177. (b) Fee, J. A. *Struct. Bonding (Berlin)* **1975**, *23*, 1. (c) Gray, H. B. *Adv. Inorg. Biochem.*, in press.
(3) Solomon, E. I.; Hare, J. W.; Gray, H. B. *Proc. Natl. Acad. Sci. U.S.A.* **1976**, *73*, 1389.
(4) Dooley, D. M.; Rawlings, J.; Dawson, J. H.; Stephens, P. J.; Andréasson, L.-E.; Malmström, B. G.; Gray, H. B. *J. Am. Chem. Soc.*, **1979**, *101*, 5038.
(5) Dawson, J. H.; Dooley, D. M.; Clark, R.; Stephens, P. J.; Gray, H. B. *J. Am. Chem. Soc.*, **1979**, *101*, 5046.
(6) (a) Solomon, E. I.; Rawlings, J.; McMillin, D. R.; Stephens, P. J.; Gray, H. B. *J. Am. Chem. Soc.* **1976**, *98*, 8046. (b) McMillin, D. R.; Holwerda, R. A.; Gray, H. B. *Proc. Natl. Acad. Sci. U.S.A.* **1974**, *71*, 1338. (c) McMillin, D. R.; Rosenberg, R. C.; Gray, H. B. *Ibid.* **1974**, *71*, 4428.
(7) (a) Markley, J. L.; Ulrich, E. L.; Berg, S. P.; Krogmann, D. W. *Biochemistry* **1975**, *14*, 4428. (b) Ugurbil, K.; Norton, R. S.; Allherhand, A.; Bersohn, R. *Ibid.* **1977**, *16*, 886.
(8) (a) Solomon, E. I.; Clendening, P. J.; Gray, H. B.; Grunthaner, F. J. *J. Am. Chem. Soc.* **1974**, *97*, 3878. (b) Wurzbach, J. A.; Grunthaner, P. J.; Dooley, D. M.; Gray, H. B.; Grunthaner, F. J.; Gay, R. R.; Solomon, E. I. *Ibid.* **1977**, *99*, 1257. (c) Thompson, M.; Whelan, J.; Zemon, D. J.; Bosnich, B.; Solomon, E. I.; Gray, H. B. *Ibid.* **1979**, *101*, 2482. (d) Hare, J. W. Ph.D. Thesis, California Institute of Technology, 1976.
(9) Colman, P. M.; Freeman, H. C.; Guss, J. M.; Murata, M.; Norris, V. A.; Ramshaw, J. A. M.; Venkatappa, M. P. *Nature (London)* **1978**, *272*, 319.
(10) Adman, E. T.; Stenkamp, R. E.; Sieker, L. C.; Jensen, L. H. *J. Mol. Biol.* **1978**, *123*, 35.
(11) Tullius, T. D.; Frank, P.; Hodgson, K. O. *Proc. Natl. Acad. Sci. U.S.A.* **1978**, *75*, 4069.
(12) Bergman, C.; Gandvik, E. -K.; Nyman, P. O.; Strid, L. *Biochem. Biophys. Res. Commun.* **1977**, *77*, 1052.
(13) Wells, J. R. E. *Biochem. J.* **1965**, *97*, 228.
(14) Ambler, R. P.; Brown, L. M. *Biochem. J.* **1967**, *109*, 784.
(15) Reinhammar, B. *Biochim. Biophys. Acta* **1970**, *205*, 35.
(16) (a) Osborne, G. A.; Cheng, J. C.; Stephens, P. J. *Rev. Sci. Instrum.* **1973**, *44*, 10. (b) Nafie, L. A.; Kelderling, T. A.; Stephens, P. J. *J. Am. Chem. Soc.*

1976, *98,* 2715.
(17) Peisach, J.; Levine, W. G.; Blumberg, W. E. *J. Biol. Chem.* **1967,** *242,* 2847.
(18) Falk, K. -E.; Reinhammar, B. *Biochim. Biophys. Acta* **1972,** *285,* 84.
(19) McFarland, T. M.; Coleman, J. E. *Eur. J. Biochem.* **1972,** *29,* 591.
(20) Blumberg, W. E.; Peisach, J. *Biochim. Biophys. Acta* **1966,** *126,* 269.
(21) Milne, P. R.; Wells, J. R. E. *J. Biol. Chem.* **1970,** 245, 1566.
(22) Tang, S. P. W.; Coleman, J. E.; Myer, Y. P. *J. Biol. Chem.* **1968,** *243,* 4286.
(23) (a) Hathaway, B. J.; Tomlinson, A. A. G. *Coord. Chem. Rev.* **1970,** *5,* 1. (b) Hathaway, B. J.; Billing, D. E. *Ibid.* **1970,** 143.
(24) Freeman, H. C. In "The Biochemistry of Copper", Peisach, J., Aisen, P., Blumberg, W. E., Eds.; Academic Press: New York, 1966.
(25) Bryce, G. F. *J. Phys. Chem.* **1966,** *70,* 3549.
(26) Corrigan, M. F.; Murray, K. S.; West, B. O.; Pilbrow, J. R. *Aust. J. Chem.* **1977,** *30,* 2455.
(27) Slade, R. C.; Tomlinson, A. A. G.; Hathaway, B. J.; Billing, D. E. *J. Chem. Soc. A* **1968,** 61.
(28) Barbucci, R.; Bencini, A.; Gatteschi, D. *Inorg. Chem.* **1977,** *16,* 2117.
(29) Hatfield, W. E.; Jones, E. R. Jr. *Inorg. Chem.* **1970,** *6,* 1502.
(30) Wood, J. S. *J. Chem. Soc. A* **1969,** 1582.
(31) Becker, C. A. L.; Meek, D. W.; Dunn, T. M. *J. Phys. Chem.* **1968,** *72,* 3588.
(32) Bernal, I.; Elliott, N.; LaLancette, R. A.; Brennan, T. "Progress in Coordination Chemistry", Cais, M., Ed.; American Elsevier: New York, 1968; p 518.
(33) Ballhausen, C. J. "Introduction to Ligand Field Theory", McGraw-Hill: New York, 1962.
(34) Dietz, R. E.; Kamimura, H.; Sturge, M. D.; Yariv, A. *Phys. Rev.* **1963,** *132,* 1559.
(35) Koster, G. F.; Dimmock, J. O.; Wheller, R. G.; Statz, H. "Properties of the Thirty-Two Point Groups", M.I.T. Press: Cambridge, Mass., 1963.
(36) Liehr, A. D. *J. Phys. Chem.* **1960,** *64,* 43.
(37) The recently prepared copper(I) complex (hydridotris(3,5-dimethyl-1-pyrazoyl)borato)(*p*-nitrobenzenethiolato)cuprate(I) has an elongated trigonal geometry plus an off-axis tilt of the metal–sulfur bond (Thompson, J. S.; Marks, T. J.; Ibers, J. A. *Proc. Natl. Acad. Sci. U.S.A.* **1977,** *74,* 3114). Although the analogous copper(II) complex was suggested to have a similar structure, based on vibrational data, the EPR spectrum yields $g_{\parallel} = 2.286$ and $g_{\perp} = 2.067$, in contrast to the *g*-value predictions of Figure 10.
(38) One of the proposals for the blue copper site in poplar plastocyanin is that two sulfur atoms, one nitrogen, and the copper ion are arranged trigonally in one plane, with the other nitrogen atom perpendicular to this plane; this structure has C_s symmetry, with the mirror plane containing both nitrogen atoms and the copper ion (Colman, P. M.; Freeman, H. C.; Guss, M. G.; Murata, M.; Norris, V. A.; Ramshaw, J. A. M.; Venkatappa, M. P. *Proc. Int. Congr. Photosynth., 4th* **1977,** 810). We have calculated the crystal field matrix elements for this structure according to a standard method (*J. Chem. Educ.* **1964,** *41,* 257), using the real d-electron basis set. The spin–orbit matrix elements for the real basis set are given by Ballhausen.[33] The angle between the two sulfur atoms was kept as a variable and the radial parameters were assumed equal. The nitrogen radial parameters were assumed to be related by the ratio of the two Cu–N bond lengths *a*. The T_3 energy matrix for the C_s double group is

$$\begin{vmatrix} {}^{+}(x^2-y^2) & {}^{+}(z^2) & {}^{+}(xy) & {}^{-}(xz) & {}^{-}(yz) \\ H_{11}-E & H_{13} & i\lambda & \lambda/2 & -i\lambda/2 \\ H_{13} & H_{33}-E & 0 & -\sqrt{3}\lambda/2 & -i\sqrt{3}\lambda/2 \\ -i\lambda & 0 & H_{55}-E & i\lambda/2 & \lambda/2 \\ \lambda/2 & -\sqrt{3}\lambda/2 & -i\lambda/2 & H_{22}-E & -i\lambda/2 \\ i\lambda/2 & i\sqrt{3}\lambda/2 & \lambda/2 & i\lambda/2 & H_{44}-E \end{vmatrix} = 0$$

where

$H_{11} = 2(3\sin^2(\theta/2) - 1)\,Ds^S - (1 + a^3)Ds^N - [3/4(35/3\sin^4(\theta/2) - 10\sin^2(\theta/2) + 1)\,Dt^S + (1 + a^5)Dt^N]$

$H_{22} = [-(3\sin^2(\theta/2) - 1) - 3\cos^2(\theta/2)]Ds^S + (-1 + 2a^3)Ds^N - [-3(35/3\sin^4(\theta/2) - 10\sin^2(\theta/2) + 1) + 5\cos^2(\theta/2)(7\sin^2(\theta/2) - 1)]\,Dt^S + (4 - a^5)Dt^N$

$H_{33} = -2(3\sin^2(\theta/2) - 1)Ds^S + (1 + a^3)Ds^N - (9/2)(35/3\sin^4(\theta/2) - 10\sin^2(\theta/2) + 1)Dt^S - (9/4)(1 + a^5)Dt^N$

$H_{44} = [-(3\sin^2(\theta/2) - 1) + 3\cos^2(\theta/2)]Ds^S + (2 - a^3)\,Ds^N - [-3(35/3\sin^4(\theta/2) - 10\sin^2(\theta/2) + 1) - 5\cos^2(\theta/2)(7\sin^2(\theta/2) - 1)]Dt^S - (1 - 4a^5)Dt^N$

$H_{55} = 2(3\sin^2(\theta/2) - 1)Ds^S - (1 + a^3)Ds^N - [3/4(35/3\sin^4(\theta/2) - 10\sin^2(\theta/2) + 1) - 35/4\cos^4(\theta/2)]Dt^S + 4(1 + a^5)Dt^N$

$H_{13} = 2\sqrt{3}\cos^2(\theta/2)\,Ds^S + \sqrt{3}(1 - a^3)Ds^N - 5\sqrt{3/2}\cos^2(\theta/2)(7\sin^2(\theta/2) - 1)Dt^S + 5\sqrt{3/4}(1 - a^5)Dt^N$

The ground-state wave functions derived from this matrix and the Γ_4 matrix by diagonalization will have the form

$$\Gamma_3{}^{gs} = a({}^{+}x^2 - y^2) + b({}^{+}z^2) + c({}^{+}xy) + d({}^{-}xz) + e({}^{-}yz)$$

$$\Gamma_4{}^{gs} = a'({}^{-}x^2 - y^2) + b'({}^{-}z^2) + c'({}^{-}xy) + d'({}^{+}xz) + e'({}^{+}yz)$$

where the coefficient may be complex. Operating on these wave functions with the Zeeman operator yields the following expressions for the *g* values:

$$g_z = 2[a^*a + b^*b + c^*c - d^*d - e^*e - 2ika^*c + 2ikc^*a - ikd^*e + ike^*d]$$

$$g_y = 2[(-ia^*a' - ib^*b' - ic^*c' + id^*d' + ie^*e' + ika^*d' - i\sqrt{3}kb^*d' + ikc^*e' - ikd^*a' + i\sqrt{3}kd^*b' - ike^*c')(iaa'^* + ibb'^* + icc'^* - idd'^* - iee'^* + i\sqrt{3}kbd'^* - ikce'^* + ikda'^* - i\sqrt{3}kdb'^* + ikec'^*)]^{1/2}$$

$$g_x = 2[a^*a' + b^*b' + c^*c' + d^*d' + e^*e' - ikc^*d' + ika^*c' + i\sqrt{3}kb^*e' + ikd^*e' - i\sqrt{3}ke^*b' - ike^*a')(aa'^* + bb'^* + cc'^* + dd'^* + ee'^* + ikcd'^* - ikae'^* - i\sqrt{3}kbe'^* - ikde'^* + i\sqrt{3}keb'^* + ikea'^*)]^{1/2}$$

For $Ds^S = 1200\ cm^{-1}$, $Dt^S = 300\ cm^{-1}$, $Ds^N = 1500\ cm^{-1}$, $Dt^N = 375\ cm^{-1}$, $a = 1.1$, $\theta = 120.0$, and $k = 0.6$, two transitions are centered around 5000 cm^{-1} and two around 10 000 cm^{-1}, the approximate energy splitting observed in the blue proteins. For this set of parameters $g_z = 1.79$, $g_y = 1.99$, and $g_x = 1.98$. With such a large set of parameters to fit only two data points, this combination is hardly unique; however, varying the parameters over physically reasonable ranges always predicts $g_z < g_x, g_y \sim 2.0$, in contrast to the experimental results[2] for blue copper.
(39) Both crystal field[40,41] and angular overlap[42] calculations have been performed previously on chlorocuprates. The distortion angle $\theta = 2\beta$ has been empirically related to d–d transition energies by Willett et al.[43] and Harlow et al.[44] Our calculation gives the same orbital energy order in the square-planar limit ($d_{x^2-y^2} > d_{xy} > d_{z^2} > d_{xz}, d_{yz}$) as obtained by Smith.[42] The polarized spectra of a single crystal containing square-planar $CuCl_4^{2-}$ have been measured (Cassidy, P.; Hitchman, M. A. *J. Chem. Soc., Chem. Commun.* **1975,** 837) and two different interpretations have been proposed (Cassidy, P.; Hitchman, M. A. *Inorg. Chem.* **1977,** *16,* 1568). The favored interpretation gives $d_{x^2-y^2} > d_{xy} > d_{xz}, d_{yz} > d_{z^2}$, but other energy-level orderings cannot be excluded with confidence, owing to the complex nature of the vibronic analysis problem.
(40) Day, P. *Proc. Chem. Soc., London* **1964,** 18.
(41) Hatfield, W. E.; Piper, T. S. *Inorg. Chem.* **1964,** *3,* 841.
(42) (a) Smith, D. W. *J. Chem. Soc. A* **1970,** 2900. (b) *Struct. Bonding (Berlin)* **1972,** *12,* 49.
(43) Willett, R. D.; Jaugen, J. A.; Lebsack, J.; Morrey, J. *Inorg. Chem.* **1974,** *13,* 2510.
(44) Harlow, R. L.; Wells, W. J. III; Watt, G. W.; Simonsen, S. H. *Inorg. Chem.* **1975,** *14,* 1768.
(45) Yokoi, H.; Addison, A. W. *Inorg. Chem.* **1977,** *16,* 1341.
(46) Murakami, Y.; Matsuda, Y.; Sakata, K. *Inorg. Chem.* **1971,** *10,* 1728.
(47) Sakaguchi, U.; Addison, A. W. *J. Am. Chem. Soc.* **1977,** *99,* 5189.
(48) Glick, M. D.; Gavel, D. P.; Diaddario, L. L.; Rorabacher, D. B. *Inorg. Chem.* **1976,** *15,* 1190.
(49) Rhombic splitting of $g_{\perp}$ is the only spectroscopic evidence for lower symmetry in stellacyanin. Assigning the 5250-cm^{-1} band as the higher energy component of a pair derived from $^2B_2 \rightarrow {}^2E$, the value of the orbital reduction factor k_x is calculated to be 0.08. Assuming $k_y = k_x$, the unobserved partner of the split $^2B_2 \rightarrow {}^2E$ set is predicted to have a transition energy of 1720 cm^{-1}. Using the mean of this splitting as the energy of the parent ^2E state, corrected D_{2d} ligand field parameters are $Ds = 690$ and $Dt = 475\ cm^{-1}$. In the axial model $\beta = 58.5°$ is required to give $\Delta W(^2A_{1g} - {}^2B_{1g}) \sim 24\,000\ cm^{-1}$ in the square-planar limit, and the highest energy d–d transition in stellacyanin is predicted to be at 10 460 cm^{-1}. Thus the specific inclusion of the rhombic distortion does not upset any of the main conclusions based on the higher symmetry (D_{2d}) model.
(50) Brill, A. S.; Bryce, G. F.; Maria, H. J. *Biochim. Biophys. Acta* **1968,** *154,* 342.
(51) Malmstrom, B. G.; Reinhammar, B.; Vanngard, T. *Biochim. Biophys. Acta* **1970,** *205,* 48.
(52) Bates, C. A.; Moore, W. S.; Standley, K. J.; Stevens, K. W. H. *Proc. Phys. Soc., London* **1962,** *79,* 73.
(53) Sailasuta, N.; Anson, F. C.; Gray, H. B. *J. Am. Chem. Soc.* **1979,** *101,* 455.
(54) Gillard, R. D. In "Physical Methods in Advanced Inorganic Chemistry", Hill, H. A. O., Day, P., Eds.; Interscience: New York, 1968.
(55) Amundsen, A. R.; Whelan, J.; Bosnich, B. *J. Am. Chem. Soc.* **1977,** *99,* 6730.
(56) (a) Miskowski, V. M.; Thich, J. A.; Solomon, R.; Schugar, H. J. *J. Am. Chem. Soc.* **1976,** *98,* 8344. (b) Hughey, J. L. IV; Fawcett, T. G.; Rudich, S. M.; Lalancette, R. A.; Potenza, J. A.; Schugar, H. J. *Ibid.* **1979,** *101,* 2617.
(57) Miskowski, V. M.; Gray, H. B. *Inorg. Chem.* **1975,** *14,* 401.
(58) Ferris, N. S.; Woodruff, V. H.; Rorabacher, D. B.; Jones, T. D.; Ochrymowycz, L. A. *J. Am. Chem. Soc.* **1978,** *100,* 5939.
(59) However, note that there is a 24 500-cm^{-1} *A* term in the MCD spectrum of azurin; this feature may be assigned to the Soret transition of cytochrome impurity. Such impurities are often found in *P. aeruginosa* azurin preparations.
(60) Lax, M. *J. Chem. Phys.* **1952,** *20,* 1752.
(61) Miskowski, V. M.; Tang, S. -P. W.; Spiro, T. G.; Shapiro, E.; Moss, T. H. *Biochemistry* **1975,** *14,* 1244.
(62) Siiman, O.; Young, N. M.; Carey, P. R. *J. Am. Chem. Soc.* **1974,** *96,* 5583.
(63) Holwerda, R. A.; Wherland, S.; Gray, H. B. *Annu. Rev. Biophys. Bioeng.* **1976,** *5,* 363.
(64) Wherland, S.; Gray, H. B. "Biological Aspects of Inorganic Chemistry", Addison, A. W., Cullen, W. C., Dolphin, D. W., James, B. R., Eds.; Wiley: New York, 1977; pp 289–368.